Electro-optical Parameters of Bond Polarizability Model for Aluminosilicates

ARTICLE *in* THE JOURNAL OF PHYSICAL CHEMISTRY A · MAY 2006

Impact Factor: 2.69 · DOI: 10.1021/jp060151+ · Source: PubMed

3 AUTHORS, INCLUDING:

Konstantin Smirnov
Volgograd State University
70 PUBLICATIONS **1,063** CITATIONS
SEE PROFILE

Poonam Tandon
University of Lucknow
206 PUBLICATIONS **973** CITATIONS
SEE PROFILE

Electro-optical Parameters of Bond Polarizability Model for Aluminosilicates

Konstantin S. Smirnov,*,† Daniel Bougeard,† and Poonam Tandon‡

Laboratoire de Spectrochimie Infrarouge et Raman, UMR 8516 CNRS-USTL, Université des Sciences et Technologies de Lille, 59655 Villeneuve d'Ascq Cédex, France, and Physics Department, Lucknow University, Lucknow 226 007, India

Received: January 9, 2006

Electro-optical parameters (EOPs) of bond polarizability model (BPM) for aluminosilicate structures were derived from quantum-chemical DFT calculations of molecular models. The tensor of molecular polarizability and the derivatives of the tensor with respect to the bond length are well reproduced with the BPM, and the EOPs obtained are in a fair agreement with available experimental data. The parameters derived were found to be transferable to larger molecules. This finding suggests that the procedure used can be applied to systems with partially ionic chemical bonds. The transferability of the parameters to periodic systems was tested in molecular dynamics simulation of the polarized Raman spectra of α-quartz. It appeared that the molecular Si−O bond EOPs failed to reproduce the intensity of peaks in the spectra. This limitation is due to large values of the longitudinal components of the bond polarizability and its derivative found in the molecular calculations as compared to those obtained from periodic DFT calculations of crystalline silica polymorphs by Umari et al. (*Phys. Rev. B* **2001**, *63*, 094305). It is supposed that the electric field of the solid is responsible for the difference of the parameters. Nevertheless, the EOPs obtained can be used as an initial set of parameters for calculations of polarizability related characteristics of relevant systems in the framework of BPM.

1. Introduction

Aluminosilicates are one of the most important class of chemical compounds due to their abundance in the nature and wide use in many industrial applications. Among the variety of experimental techniques used to characterize these systems, methods of vibrational spectroscopy, and the Raman spectroscopy in particular, play an important role in the description of local structure and of bonding at the atomic scale. The complexity of aluminosilicate structures makes it necessary to use theoretical tools for the interpretation of the experimental data. For systems with large numbers of atoms in the unit cell and low symmetry, as the aluminosilicates often are, the first-principle calculations of the vibrational spectra are often prohibitive and the methods based on the model of effective potentials remain an indispensable tool for studying their vibrational dynamics. The normal-mode analysis for molecules and the lattice dynamics method for solids are perhaps most widely used computational techniques for this purpose. Another method providing a detailed information about the behavior of system at the microscopic level is molecular dynamics (MD).

To calculate the Raman scattering intensity, all these techniques need a parametric model describing the variation of the system's polarizability upon variation of the atomic coordinates and such a model, which is almost exclusively used for this purpose, is the bond polarizability model (BPM).[1−3] The BPM has widely been employed in the calculations of Raman spectra of various aluminosilicates such as glasses,[4−8] zeolites,[9,10] and clays[11,12] as well as of other materials such as fullerenes,[13] Si nanowires,[14] carbon nanotubes,[15] or minerals.[16] (The list of references is, of course, not exhaustive.) Results of these studies indicate a good general agreement of the BPM calculated and experimental spectra. Recently, Umari et al.[17] showed that the BPM reproduced the Raman scattering intensities derived from periodic DFT calculation of two silica polymorphs with an average error of 15%. The authors found a good transferability of BPM parameters derived for α-quartz to a cristobalite polymorph.

Despite such a wide use of the bond polarizability model the absolute values of BPM parameters are only known for some simple systems such as alkanes.[18,19] For aluminosilicate structures the parameters were often chosen in an arbitrary way or were fitted so that the calculated spectra reproduced the experimental ones. Recently, an approach for deriving the electro-optical parameters (EOPs) of BPM from results of quantum-chemical calculations was proposed.[19] With this approach, EOPs for alkanes were obtained and their values were found to be in a good agreement with those determined from the experimental absolute Raman scattering intensities of saturated hydrocarbons. Hence, one might hope that the procedure used in ref 19 could be applied to obtain BPM parameters for more complex systems and indeed, such an approach was very recently used to study the Raman spectra of BN nanotubes.[20] The present paper pursues two goals. The first one is to test the feasibility of the approach for aluminosilicates, which have a type of bonding different from that in the saturated hydrocarbons. The second aim is to verify the transferability of parameters obtained on molecular models to periodic structures.

2. Model and Methods

BPM Model and Derivation of Electro-optical Parameters. The BPM represents the polarizability tensor **A** of system as the sum of bond polarizabilities

$$\mathbf{A} = \sum_i a_i \qquad (1)$$

* Corresponding author. E-mail: Konstantin.Smirnov@univ-lille1.fr.
† Université des Sciences et Technologies de Lille.
‡ Lucknow University.

10.1021/jp060151+ CCC: $33.50
Published on Web 03/16/2006

where $\mathbf{a}_i$ stands for the polarizability tensor of bond i in fixed Cartesian frame. The tensor $\mathbf{a}_i$ can be written as

$$\mathbf{a}_i = \mathbf{R}_i \alpha_i \mathbf{R}_i^{-1} \quad (2)$$

where α_i is the bond polarizability tensor in its principal axes and $\mathbf{R}_i$ is a rotation matrix between the bond principal and the Cartesian frames. To obtain the elements of the $\mathbf{R}_i$ matrix, it is generally supposed that (i) one of the principal axes coincides with the bond direction and (ii) there is no preferential orientation perpendicular to the bond. The latter assumption is known as the cylindrical bond model. Hence, the tensor α_i has two principal components, which are the longitudinal (L) and the transversal (T) bond polarizabilities. In the zero-order BPM, which is used in the present study, the components of α_i are expanded in a Taylor series with respect to the variation of length Δr_i of the bond i

$$\alpha_s(i) = \alpha_s^0(i) + \alpha_s'(i)\Delta r_i + ... \quad (3)$$

where $\alpha_s'(i) \equiv \partial\alpha_s(i)/\partial r_i$, the index s indicates for the polarizability component (s = L, T), and zero denotes the equilibrium value. The bond polarizability tensor and its variation with the bond length are therefore described by four parameters α_L^0, α_T^0, α_L' and α_T' , which are known as the equilibrium and valence bond electro-optical parameters, respectively.

From eqs 1−3 it follows that the Cartesian components A_{pq}^0 ($p, q = x, y, z$) of the polarizability tensor of system in the equilibrium and the derivatives A_{pq}' of the components with respect to the length of a single bond i can be written as

$$A_{pq}^0 = \sum_s \sum_k \sum_{i \in k} \alpha_s^0(k)\, P_s(i)\, Q_s(i) \quad (4)$$

$$A_{pq}' = \sum_s \alpha_s'(k_i)\, P_s(i)\, Q_s(i) \quad (5)$$

where the index k runs over types of bonds in the system and $P_s(i)$ and $Q_s(i)$ are the elements of the matrix $\mathbf{R}_i$. One sees that these components are the linear functions of the EOPs and the parameters can therefore be derived by a linear fitting procedure using databases of the A_{pq}^0 and A_{pq}' values for molecules with well-defined geometry.[19]

To obtain the electro-optical parameters of aluminosilicates, the databases of A_{pq}^0 and A_{pq}' values were generated by quantum-chemical calculations of the 26 molecular models listed in Table 1. The calculations were carried out at the B3LYP/6-311+G(3df,2p) level with the Gaussian 03 program.[21] The geometry of the molecules was first optimized without any symmetry constraints and then followed by the calculation of the polarizability tensor. All elements of these tensors constituted the A_{pq}^0 database. The databases of A_{pq}' values for bonds of each type were generated by stretching all nonequivalent bonds of a given type by $\Delta r = 0.01$ Å. The linear least-squares fit was performed with the use of singular value decomposition method.[22]

Testing the EOPs Parameters. The equilibrium EOPs obtained with the procedure described above were tested in the calculation of the polarizability tensor of two molecular models, $Si_2AlO_4H_7$ and $Si_5O_4H_{12}$ (Figure 1), whose size exceeds that of the molecules used to generate the A_{pq}^0 database. The tensors computed with the BPM were compared with those issued from the B3LYP/6-311+G(3df,2p) calculations. In addition, the optical dielectric constant of α-quartz structure was calculated and compared with the experimental value.

TABLE 1: Molecules Used in the DFT Calculations

	database					
		A_{pq}'				
molecule	A_{pq}^0	O−H	Al−H	Al−O	Si−H	Si−O
AlH_2OH	•	•	•	•		
AlH_3	•		•			
$AlH(OH)_2$	•	•	•	•		
$Al(OH)_3$	•	•		•		
$H_2AlOSiH_2OH$	•	•	•	•	•	•
$H_2AlOSiH(OH)_2$	•	•	•	•	•	•
$H_2AlOSi(OH)_3$	•	•	•	•		•
H_2O	•					
$H_3SiOAlH_2$	•		•	•	•	•
$H_3SiOSiH_2OH$	•	•			•	•
$H_3SiOSiH_3$	•				•	•
$H_3SiOSiH(OH)_2$	•	•			•	•
$H_3SiOSi(OH)_3$	•	•			•	•
$HOHAlOSiH_2OH$	•	•	•	•	•	•
$HOHAlOSiH_3$	•	•	•	•	•	•
$HOHAlOSiH(OH)_2$	•	•	•	•	•	•
$HOHAlOSi(OH)_3$	•	•	•	•		•
$(OH)_2AlOSiH_2OH$	•	•		•	•	•
$(OH)_2AlOSiH_3$	•	•		•	•	•
$(OH)_2AlOSiH(OH)_2$	•	•		•	•	•
$(OH)_2AlOSi(OH)_3$	•	•		•		•
$SiH_2(OH)_2$	•	•			•	•
SiH_3OH	•	•			•	•
SiH_4	•				•	
$SiH(OH)_3$	•	•			•	•
$Si(OH)_4$	•	•				•
no. of entries	150	162	96	150	126	222

The complete set of EOPs including both equilibrium and valence parameters was submitted to two tests. The first one consisted of the calculation of the variation of the mean molecular polarizability and the anisotropy of the polarizability in the normal modes of the $Si_2AlO_4H_7$ molecule. The normal-mode analysis was performed in B3LYP/6-311+G(3df,2p) calculation and the polarizability tensors of molecular structures distorted according to the atomic displacements in 36 normal modes were calculated with both the DFT and BPM. The second test included the molecular dynamics simulations of the polarized Raman spectra of α-quartz. The MD simulation box consisted of 4 × 4 × 4 unit cells, and the periodic boundary conditions were applied to the box along the crystallographic axes. The c and b crystallographic axes coincided with the z and y axes of the Cartesian frame, respectively. Initial atomic positions and the unit cell parameters were taken from ref 23. Interactions between atoms of the solid were described by a generalized valence force field model by Lazarev and Mirgorodsky.[24] The force field was specially tuned to reproduce the IR spectrum, the elastic and piezoelectric constants, and the compressibility of the solid. Values of the force field parameters can be found elsewhere.[24] The classical equations of atomic motion were integrated with the velocity Verlet algorithm with time-step of 1 fs. A typical MD run consisted of 20 ps equilibration stage and 41.96 ps production stage. The atomic coordinates and velocities were saved each tenth step during the last 40 960 time-steps. The simulations were performed in the microcanonical ensemble for the temperature 300 K.

The Raman spectrum was calculated as the spectrum of fluctuations of the time-dependent polarizability tensor $\mathbf{A}(t)$ of the system[25−27]

$$\lambda_s^4 \left(\frac{d^2\sigma}{d\omega\, d\Omega} \right) = (2\pi)^4 \int dt\, e^{i\omega t} \langle \mathbf{A}(t) \cdot \mathbf{A}(0) \rangle \quad (6)$$

where the left-hand side stands for the differential scattering

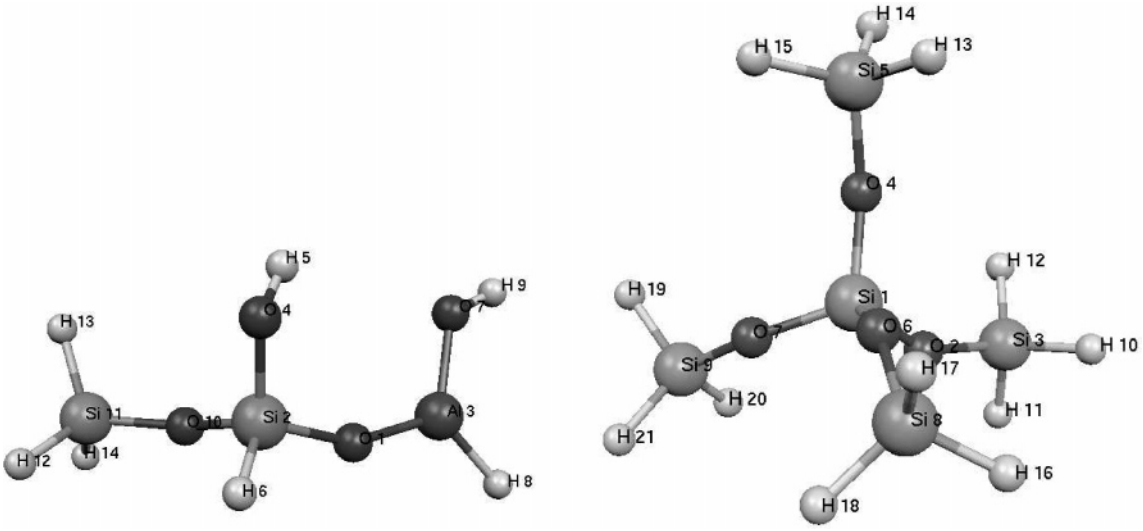

Figure 1. $Si_2AlO_4H_7$ (left) and $Si_5O_4H_{12}$ (right) molecular models used in the validation set.

cross-section for scattering into frequency range dω and solid angle dΩ. The cross-section is amplified by the factor λ_s^4, λ_s being the wavelength of scattered radiation. Raman spectrum of crystal in specific experimental geometry, i.e., the direction and the polarization of the incident and scattered radiation, can be calculated by (6) from the components of the polarizability tensor **A**. Thus, assuming that the axes of the laboratory frame coincide with the Cartesian axes of MD simulation box, the Raman spectrum measured in the $x(zx)y$ geometry can be computed as the spectrum of fluctuations of the $A_{zx}(t)$ tensor component. The calculated spectra were multiplied by a quantum correction factor obtained in the double harmonic approximation[27]

$$\frac{\beta\hbar\omega}{1-\exp(-\beta\hbar\omega)} \tag{7}$$

where $\beta \equiv 1/k_BT$ with k_B and T denoting the Boltzmann constant and the temperature, respectively. Furthermore, the intensity in the spectra was scaled by the factor $(\lambda_0/\lambda_s)^4$ with the incident radiation wavelength $\lambda_0 = 632.8$ nm and the scattered radiation wavelength λ_s corresponding to the Stokes scattering. The spectra presented below were obtained as the average of spectra computed from 100 MD trajectories started from different initial conditions.

Experiment. The calculated spectra were compared with the polarized Raman spectra of α-quartz measured on LabRAM confocal spectrometer (HORIBA Jobin Yvon S. A. S., France) using the backscattering geometry. The Raman effect was excited with the 632.8 nm line of He−Ne laser. A rotating polarizer (half-wave plate) was placed in the laser beam path to discriminate two polarizations of the exciting radiation. The scattered radiation was analyzed by positioning the analyzer either parallel or perpendicular to the electric field vector of the exciting light. An α-quartz sample in the form of a plate was used. The sample had the *c* axis in the plane of the plate surface. The laser beam was focused on the plate surface to minimize rotation of the polarization by the sample. The *c* crystallographic axis is assumed to be the *z* axis of the laboratory frame.

3. Results

Equilibrium EOPs. The equilibrium EOPs derived by the fit of the DFT calculated components A^0_{pq} with eq 4 are presented in Table 2. Figure 2 shows the correlation graph between the A^0_{pq} values obtained in the DFT calculations and those fitted with the BPM using the EOPs. A good agreement between the first-principles and BPM results (correlation coeffcient of 0.999) confirms that the polarizability of molecules can successfully be constructed as the sum of bond polarizabilities.

The right-hand part of Table 2 reports experimental values of the bond EOPs found in the literature. Note that the small

TABLE 2: Equilibrium Electro-optical Parameters (in Å^3) for Aluminosilicates

	this work		experiment	
bond k	$\alpha_L^0(k)$	$\alpha_T^0(k)$	$\alpha_L^0(k)$	$\alpha_T^0(k)$
O−H	0.668 (0.035)[a]	0.605 (0.028)	0.7590 (0.0301)	0.7232 (0.0155)[d]
Al−H	1.916 (0.037)	1.393 (0.024)		
Si−H	1.401 (0.166)	0.993 (0.084)	1.70	0.90[e]
			1.78	0.88[f]
Al−O	1.751 (0.037)	0.784 (0.026)		
Si−O	1.524 (0.165)	0.473 (0.085)	1.07	0.66[f]
SE[b]	0.186			
cos η[c]	0.9995			

[a] Values in brackets are the statistical uncertainties. [b] Standard error of A_{pq} values. [c] The cosine of the angle between the vectors of the DFT calculated and BPM fitted A_{pq} values. [d] Reference 28. [e] Reference 32. [f] Reference 50.

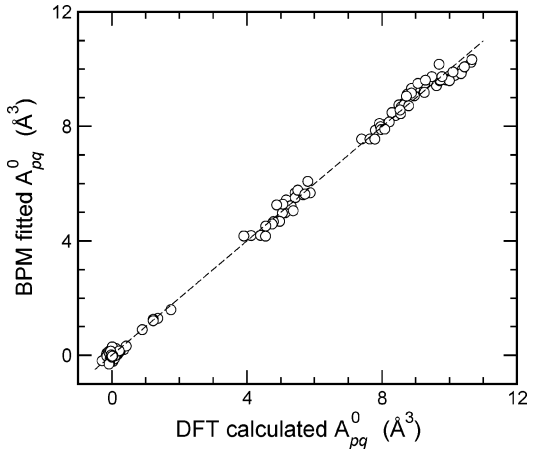

Figure 2. Correlation graphs between the DFT calculated with and BPM fitted components of the polarizability tensors of the molecules listed in Table 1. Dashed line indicates perfect correlation.

TABLE 3: Valence Electro-optical Parameters (in Å²) for Aluminosilicates

bond k	$\alpha'_L(k)$	$\alpha'_T(k)$	SE[a]	cos η[a]
O−H	2.512 (0.059)[a]	0.425 (0.040)	0.286	0.9615
Al−H	3.288 (0.079)	0.917 (0.053)	0.093	0.9978
Si−H	3.097 (0.068)	0.635 (0.046)	0.133	0.9944
Al−O	3.066 (0.060)	0.708 (0.041)	0.227	0.9847
Si−O	3.127 (0.050)	0.612 (0.034)	0.278	0.9770
	Refined Parameters			
Al−O(H)	2.562 (0.087)	0.743 (0.058)	0.120	0.9940
Al−O(Al,Si)	3.527 (0.083)	0.714 (0.058)	0.143	0.9954
Si−O(H)	2.499 (0.074)	0.589 (0.049)	0.159	0.9881
Si−O(Al,Si)	3.676 (0.068)	0.693 (0.047)	0.161	0.9946

[a] See footnotes to Table 2.

calculated anisotropy of the O−H bond polarizability tensor is in a good agreement with the experimental data by Murphy[28] obtained for H_2O molecule. The comparison of the Si−O and Si−H bonds bond polarizability components obtained in the present work with the literature data shows a fair agreement, especially taking into consideration large statistical uncertainties of the EOPs for the bonds. The analysis of Table 2 indicates that the anisotropy of the bond polarizabilities follows the sequence

$$\gamma_{SiO} > \gamma_{AlO} > \gamma_{AlH} > \gamma_{SiH} > \gamma_{OH}$$

which correlates with the decrease of length of the bonds. The only inversion in this series occurs for the Si−O and Al−O bonds, $\gamma_{SiO} = 1.051\ (0.246)$ Å³ and $\gamma_{AlO} = 0.967\ (0.045)$ Å³, whereas the former bond is horter than the latter. However, the difference of the anisotropies of 0.084 Å³ is smaller than the uncertainty of the γ_{SiO} value, and therefore the inversion cannot be considered as statistically meaningful.

Valence EOPs. The values of the valence EOPs $\alpha_s'(k)$ obtained by fitting the results of the first-principle calculations with eq 5 are reported in the upper part of Table 3. Figure 3 shows the correlation graphs between components of the derivative of tensor of molecular polarizability with respect to the length of the Si−H and Si−O bonds of the molecules. The analysis of Figure 3 and Table 3 demonstrates that the BPM performs well for the polarizability derivatives with respect to the length of Al−H and Si−H bonds, whereas a relatively low correlation was obtained for the derivatives with respect to the length of O−H, Al−O, and Si−O bonds.

These results suggest that there may exist other factors affecting the applicability of the zero-order BPM for the O−H, Al−O, and Si−O bonds. Thus, one can suppose that values of the $\alpha'_s(k)$ parameters for these bonds can be dependent on the location and orientation of the bonds in molecules.[29] Furthermore, one can imply that the EOPs depend on the bond length, as the Si−O and Al−O bond-stretching force constants do.[30,31] Figure 4 presents a plot of the α'_s(Si−O) parameters vs the length of the Si−O bond. Despite the fact that the length of this bond has the largest variation in the molecules studied ($\Delta r_{Si-O} = 0.047$ Å), no systematic dependence of the parameters on the bond length can be inferred from the plot. (For comparison, the Si−O bond-stretching force constant would vary by about 25%.) On the other hand, the α'_L(Si−O) parameters reveal an apparent dependence on the nature of the second neighbor of the oxygen atom (Figure 4). Thus, the polarizability derivative of the Si−O bond of silanol groups has the longitudinal component about 30% smaller than that of Si−O bond in the SiOSi or SiOAl bridges. The same trend was found for the α'_L parameter of the Al−O bond. It is noteworthy that the transversal α'_T components of both bonds are virtually not influenced by oxygen's environment. Hence, a separate fit taking into account the environment of O atom in the Al−O and Si−O bonds was carried out. The resulting EOPs are reported in the lower part of Table 3 as refined parameters, the corresponding correlation graph for the A'_{pq} derivatives with respect to the Si−O bond length are presented in Figure 5. Both the figure and the table show that the model taking into account the environment of oxygen atom in the bonds improves the correlation of the BPM results with the DFT data. On the other hand, such a model for the O−H bond fails to get a better description of the first-principle results by the BPM.

A little is known about the absolute values of the valence EOPs. From the experimental Raman spectra of the SiH_4 molecule, Armstrong and co-workers[32] have derived values of the longitudinal $\alpha'_L = 2.75$ Å² and transversal $\alpha'_T = 0.70$ Å² components of the derivative of Si−H bond polarizability. The corresponding EOPs reported in Table 3 differ at most by 10% from these values. Lupinneti and Gough[33] calculated the derivative of mean polarizability $\bar{\alpha}' = {}^1/_3(\alpha'_L + 2\,\alpha'_T)$ of Si−H bond in silanes in the range 1.28−1.99 Å². The value of $\bar{\alpha}' = 1.456$ Å² obtained in the present work is within these limits and close to the experimental value $\bar{\alpha}' = 1.38$ Å².[32]

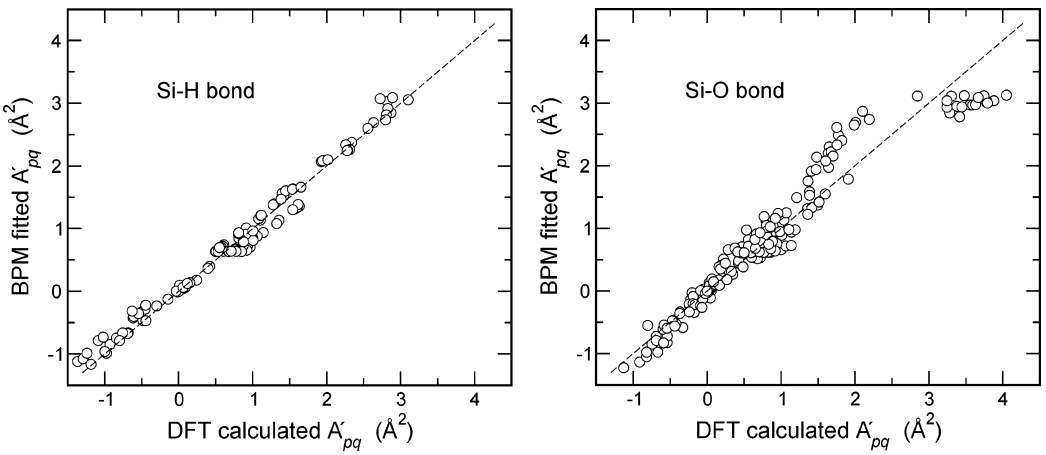

Figure 3. Correlation graphs between the DFT calculated with and BPM fitted components of the tensor of polarizability derivatives with respect to the Si−H (left pannel) and Si−O (right pannel) bond lengths of the molecules listed in Table 1. Dashed lines indicate perfect correlation.

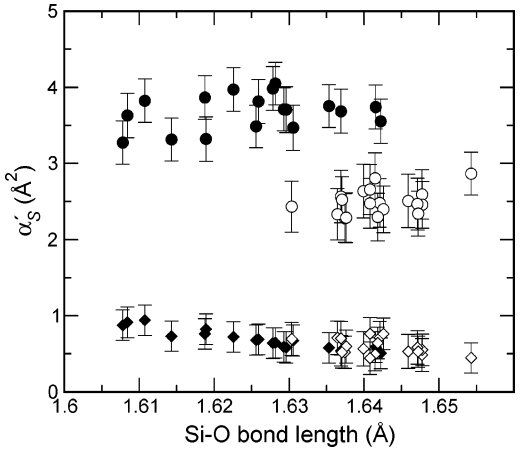

Figure 4. Correlation between the derivatives of longitudinal (circles) and transversal (diamonds) Si−O bond polarizabilities with the Si−O bond length. Open and filled symbols denote Si−O(H) and Si−O(Al,-Si) bonds, respectively.

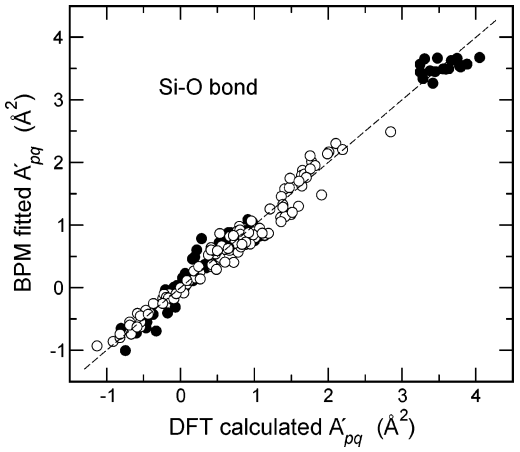

Figure 5. Correlation graph between the calculated and fitted components A'_{pq} of the tensor of polarizability derivative with respect to the Si−O bond length. Open and filled symbols stand for the separate fits for the Si−O(H) the Si−O(Al,Si) bonds, respectively.

Using the experimental relative Raman intensities of $H_8Si_8O_{12}$ molecule and taking the Si−O bond anisotropy γ_{SiO} equal to 1.00 Å^3, Bornhauser and Bougeard[10] have reported values of the valence EOPs for the bond α'_L(Si−O) = 3.55 and α'_T(Si−O) = 1.00 Å^2. The values are in a good agreement with the data of present work. By the way, the value γ_{SiO} = 1.051 Å^3 in Table 2 can be considered as a posteriori confirmation of the choice of this parameter done in ref 10. Another set of valence EOPs for Si−O bond was obtained by Umari and coworkers[17] from results of periodic DFT calculations. Their parameters for the bond in α-quartz and cristobalite structures are α'_L(Si−O) = 1.573, α'_T(Si−O) = 0.778 Å^2 and α'_L(Si−O) = 1.435, α'_T(Si−O) = 0.847 Å^2, respectively.[17] The comparison of these values with the corresponding entries in Table 3 shows that the major discrepancy exists for the longitudinal EOPs, whereas the α'_T parameters do not significantly differ from each other (by 18% at most). Consequences of such a difference are discussed in the following sections in detail.

Transferability of Parameters. The transferability of the equilibrium EOPs to large molecules was tested by computing the polarizability tensor of $Si_2AlO_4H_7$ and $Si_5O_4H_{12}$ molecular models (Figure 1), which were not included in the training set of Table 1. The tensors were obtained at the B3LYP/6-311+G-(3df,2p) level and with the BPM using the geometry optimized

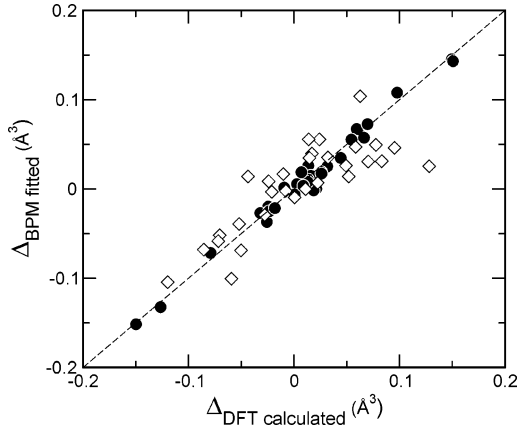

Figure 6. Correlation graph between the variation Δ of the mean polarizability $\bar{\alpha}$ (filled circles) and the polarizability anisotropy γ (open diamonds) of the $Si_2AlO_4H_7$ molecule in the normal modes, obtained in the DFT calculations and fitted with the BPM.

in the DFT calculation. For the first molecule the tensors read (in Å^3)

$$A_{DFT} = \begin{pmatrix} 14.368 & & \\ 0.171 & 11.976 & \\ 0.122 & 0.099 & 12.279 \end{pmatrix}$$

$$A_{BPM} = \begin{pmatrix} 13.539 & & \\ 0.248 & 12.214 & \\ 0.032 & 0.384 & 12.772 \end{pmatrix}$$

The maximum error in the calculation of tensor elements by the BPM is 0.829 Å^3, which is larger than the statistical uncertainty of 0.186 Å^3 of A_{pq} values in Table 2. Nevertheless, due to compensation of errors the mean polarizability of the molecule obtained with the BPM is only 0.2% smaller than the DFT calculated value (12.841 Å^3 vs 12.874 Å^3). The polarizability tensors of the $Si_5O_4H_{12}$ molecule are (in Å^3)

$$A_{DFT} = \begin{pmatrix} 20.072 & & \\ 0.018 & 19.992 & \\ -0.017 & -0.012 & 19.875 \end{pmatrix}$$

$$A_{BPM} = \begin{pmatrix} 20.208 & & \\ -0.070 & 20.125 & \\ 0.069 & 0.029 & 20.072 \end{pmatrix}$$

In this case, the maximum difference between elements of the tensors is equal to 0.197 Å^3 that is close to the statistical uncertainty of 0.186 Å^3. Again, the mean molecular polarizability is very well described by the BPM with a relative error of 0.7%.

Thereupon, the optical dielectric constant ϵ_∞ of the α-quartz structure was calculated by the BPM by using the Clausius-Mossotti formula

$$\frac{\epsilon_\infty - 1}{\epsilon_\infty + 2} = \frac{4\pi}{3}\frac{\alpha}{V} \tag{8}$$

where α is the polarizability of volume V. The calculation resulted in ϵ_∞ = 2.73, which is 15% larger than the experimental value of 2.37[34,35] and also exceeds the value ϵ_∞ = 2.443 obtained in the periodic DFT study by Umari et al.[17]

Figure 6 compares the variations of the mean molecular polarizability ($\Delta\bar{\alpha}$) and of the anisotropy of the polarizability ($\Delta\gamma$) in the normal modes of the $Si_2AlO_4H_7$ molecule that were computed in the DFT calculations and with the zero-order

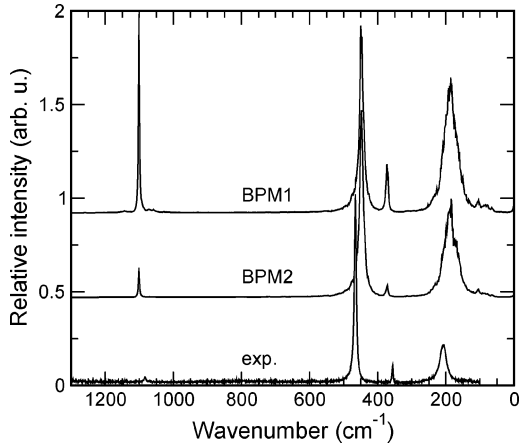

Figure 7. Experimental and MD calculated $x(zz)\bar{x}$ Raman spectra of α-quartz. The spectra are normalized at the intensity of peak at 452 cm^{-1} and shifted along the vertical axis for clarity.

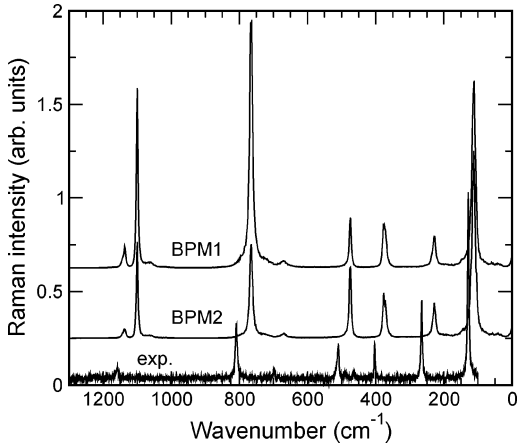

Figure 8. Experimental and calculated $x(yz)\bar{x}$ Raman spectra of α-quartz. The spectra are normalized at the intensity of peak at 123 cm^{-1} and shifted along the vertical axis for clarity.

BPM.[36] The set of EOPs used, hereafter the BPM1 set, was formed from the equilibrium EOPs of Table 2 and the refined valence EOPs of Table 3. A good correlation between the first-principle and BPM results is obtained, especially for the $\Delta\bar{\alpha}$ quantity (correlation cofficient 0.991).

The MD calculations of the Raman spectra of α-quartz were performed with the use of two sets of EOPs. The first set is the BPM1 described above. The second set, BPM2, consisted of BPM parameters obtained from the results of the periodic DFT calculations of α-quartz by Umari and co-workers.[17] As only the anisotropy of the Si−O bond polarizability was reported in that work, the mean Si−O bond polarizability was fitted in such a way to reproduce the experimental value of the optical dielectric constant of α-quartz. The resulting equilibrium EOPs of the BPM2 set are $\alpha_L^0(\text{Si}-\text{O}) = 0.948$, $\alpha_T^0(\text{Si}-\text{O}) = 0.583$ Å^3, values of the valence parameters are given above.

The Raman spectrum of α-quartz structure is well studied.[37−39] Among 24 optic modes twelve modes are Raman active comprising four modes of A_1 symmetry and eight doubly degenerate modes of E symmetry. The Raman tensor has the form[37]

$$\begin{pmatrix} A_{xx} & & \\ A_{yx} & A_{yy} & \\ A_{xx} & A_{zy} & A_{zz} \end{pmatrix} = \begin{pmatrix} a & & \\ & a & \\ & & b \end{pmatrix}_{A_1} + \begin{pmatrix} c & & \\ -c & -c & \\ -d & -d & \end{pmatrix}_{E}$$

Figure 7 shows the experimental Raman spectrum of α-quartz measured in the $x(zz)\bar{x}$ geometry and compares it with the spectra calculated from the A_{zz} polarizability tensor component. The spectra reveal vibrational modes of the A_1 symmetry (b component of the Raman tensor). The Raman spectra calculated from the A_{yz} tensor element accounting for the modes of E symmetry (d-component) are shown in Figure 8 together with the experimental spectrum measured in the $x(yz)\bar{x}$ geometry. The relative intensities of peaks in the calculated and experimental spectra are compared in Table 4. The comparison of the spectra and analysis of the table reveal that the BPM1 set overestimates the relative intensities of peaks. The BPM2 set yields a better agreement, although the intensity of the A_1 peak at 207 cm^{-1} is still too large as compared to the experiment. Note a good correlation between the peak intensities calculated with the lattice dynamics[17] and MD techniques using the BPM2 set.

TABLE 4: Relative Intensities[a] of Vibrational Modes of α-Quartz

mode[b]	ref 39 exp		ref 17 DFT		ref 17 BPM		this work exp		this work BPM1		this work BPM2	
A_1	a^2	b^2	a^2	b^2	a^2	b^2	a^2	b^2	a^2	b^2	a^2	b^2
207	484	619	696	803	801	1185	683		1028	1908	944	1330
375	38	55	70	39	1	18	55		2	112	<1	29
452	906	1000	1040	1000	1279	1000	1000		1584	1000	1344	1000
1079	2.3	31	4	33	11	62	25		70	295	9	39

mode[b]	ref 39 exp		ref 17 DFT		ref 17 BPM		this work exp		this work BPM1		this work BPM2	
E[c]	c^2	d^2	c^2	d^2	c^2	d^2	c^2	d^2	c^2	d^2	c^2	d^2
123	125	62	136	79	141	32			474	230	117	53
239	<1	28	2	27	18	10			93	40	29	9
373	11	<1	25	4	7	10			52	49	10	11
483	<1	13	<1	18	<1	17			<1	34	<1	12
673	−	−	12	6	2	1			64	17	3	3
785	<1	14	3	26	<1	28			<1	300	<1	24
1073	<1	2.7	16	14	15	14			87	116	11	14
1166	23	5.5	23	5	28	5			206	16	24	2

[a] Calculated from integrated intensities and normalized so that the intensity of peak at 452 cm $^{-1}$ = 1000. [b] The modes are identified by the frequencies (in cm^{-1}) given in ref 24. [c] The intensities of the modes of E symmetry were obtained as the mean of intensities of the longitudinal and transversal components.

4. Discussion

Results presented in the previous section permit us to conclude that the BPM sucessfully describes the polarizability of molecular models of aluminosilicates. Both the polarizability tensor and its derivatives with respect to the length of bonds correlate well with the reference data and a further improvement can be achieved by a model taking the environment of the oxygen atom in the Al−O and Si−O bonds into consideration. The resulting electro-optical parameters reasonably agree with the available experimental data. Furthermore, the polarizability tensor of molecules in the validation set as well as the variation of the mean molecular polarizability and of the anisotropy of the polarizability in the normal modes of one of the molecules are well reproduced with the BPM. The inspection of the normal modes for which the largest difference between the DFT and BPM values were calculated, showed these modes involve either (almost) pure bending motions or simultaneous variation of several internal coordinates in the same group of atoms. The discrepancy can therefore be due to the zero-order BPM used, which does not take into account the change of the bond

polarizability upon variation of the bond angles and also neglects the interaction between the coordinates. Hence, the results of the study confirm the general applicability of the BPM and of the procedure employed to derive EOPs for aluminosilicate structures.

On the other hand, the study reveals a limited transferability of the EOPs obtained in the molecular calculations to periodic systems. Thus, the optical dielectric constant of α-quartz computed with the BPM using the parameters of Table 2 exceeds the experimental value of ϵ_∞ by about 15%. This result implies that the mean polarizability of the structure is *overestimated* by the BPM using parameters derived in the molecular calculations. Furthermore, the analysis of Figures 7 and 8, and of Table 4 shows that the BPM1 set overstimates the intensity of peaks in the polarized Raman spectra of α-quartz, especially in low- and high-frequency regions. The reason for such an unsatisfactory performance of the BPM1 set becomes evident from the comparison of its parameters with those of the BPM2 set: values of the α_L and α'_L Si−O bond parameters in the former significantly exceed those in the latter. On the other hand, the α_T and α'_T parameters show much better transferability from molecules to periodic systems. The difference of the longitudinal parameters has the main impact on the anisotropies of the bond polarizability and its derivative, whereas the mean bond polarizability and its derivative are affected to a lesser extent. Thus, the mean polarizabities of the Si−O bond in the BPM1 and BPM2 sets differ by ca. 15%, whereas the difference of 280% is obtained for the bond anisotropies. Note that these are just the anisotropy of bond polarizability and its derivative that account for the intensity of the low- and high-frequency peaks in the α-quartz spectra, respectively. Again the EOPs derived from the first-principle calculations of molecules *exceed* parameters obtained in the periodic calculations and permitting to explain the experimental data.

The question about transferability of EOPs from molecules to larger systems has been adressed in studies of carbon polymorphs.[13,40,41] Thus, Bermejo et al.[40] showed that local field corrections should be taken into account while using the C−C bond EOPs derived from saturated hydrocarbons for studies of diamond. Snoke and Cardona[13] found a partial transferability of EOPs of the single and double carbon−carbon bonds in hydrocarbons to fullerens C_{60}. More recently, Guha and co-workers[41] showed that the equilibrium electro-optical parameters obtained in the studies of hydrocarbons permit a good reproduction of the static polarizability of C_{60} and C_{70}. However, being applied to the Raman intensity calculations, the molecular valence EOPs led to a notable discrepancy between the experimental and calculated intensities in a high-frequency spectral region. The authors, nevertheless, noted that the best fit parameters were close to parameters determined in hydrocarbon molecules.

A plausible explanation for the nontransferability of the molecular Si−O bond EOPs to crystalline silica structures is the influence of crystal electrostatic field. One can expect this influence to be more important for solids with partially ionic bonds such as silica as compared to covalently bonded carbon polymorphs. This hypothesis also implies that the crystal field correction should vary for different crystal structures and depend on the electronic distribution in the solid. The results of the present study indicate that such a crystal field correction can also be different for different parameters. Thus, the transversal bond polarizability parameters are close to each other in the BPM1 and BPM2 sets that is not the case for the longitudinal

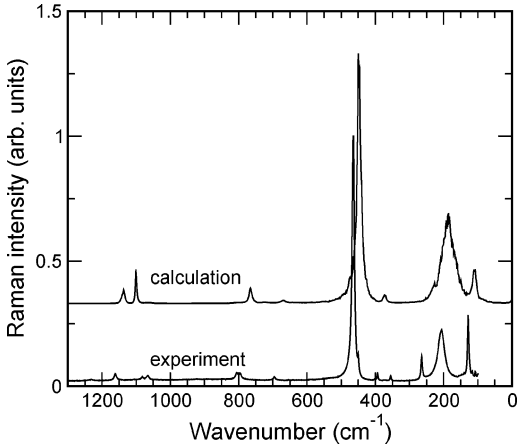

Figure 9. Experimental[49] and calculated with BPM1 parameters set Raman spectrum of α-quartz powder.

EOPs. It also worthy of note that the α'_T parameters are less sensitive to the bond environment (Figure 4).

A model taking into consideration the influence of internal field on the polarizability of molecules has been suggested by Rowell and Stein[42] and further developed by Mortensen,[43] and by Applequist and co-workers.[44] The approach is based on a dipole interaction model by Silberstein[45] and it considers the molecule as an ensemble of polarizable point dipoles. The response of the system to the external electric field, which would be just the sum of particles polarizabilities in the absence of interparticle interactions, is then modified by the dipole−dipole interactions. Apllequist et al. demonstrated that the use of the atom dipole interaction model resulted in effective atomic polarizabilities in molecules significantly smaller than the additive values.[44] A version of the model considering atoms as such polarizable dipoles was employed in calculations of the Raman spectra of molecular crystals.[46−48] However, the dipole interaction model cannot be combined with the BPM because the use of anisotropic polarizability tensors for the dipoles, which is generally the case of the bond polarizabilities, would result in erroneous symmetry of the effective bond polarizability tensors.

Despite the fact that the EOPs do not seem to be directly transferable from molecules to solids, the quality of Raman spectra calculated for disordered systems such as glasses should less be influenced by such a behavior. The Raman scattering intensity of the systems is described with the formulas

$$I_{\text{powder}} \propto 45(A'_{\text{iso}})^2 + 7(A'_{\text{aniso}})^2 \qquad (9)$$

where the first and the second term in the right-hand part stand for the contributions due to the isotropic and anisotropic parts of the derivative of polarizability tensor, respectively. One sees that the derivative of the anisotropy contributes to the intensity to a much lesser extent than that of the mean polarizability and, as the variation of EOPs has the main impact on the anisotropy, the quality of the spectra are less affected by such a behavior of the parameters. Figure 9 presents the powder Raman spectra of α-quartz[49] and shows that the relative peaks intensities in the calculated spectrum resonably agree with the experimental ones. Thus, the EOPs derived are supposed to be suitable for the modeling of the Raman spectra of disordered aluminosilicates and can also be used as a first approximation for the EOPs for crystals.

5. Conclusions

In the present work, electro-optical parameters of bond polarizabilty model for aluminosilicate structures were calculated

from the results of quantum-chemical DFT calculations of molecular models. The BPM was shown to reproduce the components of the polarizability tensor as well as the variation of the components with a change of the length of bonds in the molecules. It was found that the EOPs of Si−O and Al−O bonds are sensitive to the environment of the oxygen atom in the bonds. Therefore, the model taking the environment of the oxygen atom in the bonds into account, notably improves the correlation between the BPM and the reference quantum-chemical data. The EOPs derived are in a fair agreement with available experimental molecular parameters.

The EOPs obtained were found to be transferable to larger molecular models. Thus, the mean polarizability of two molecules of the validation set is reproduced with an error of less than 1%. The calculation of the variation of the mean molecular polarizability and of the anisotropy of the polarizability in the normal modes of one of the molecules with the zero-order BPM shows a good agreement with the reference quantum-chemical data, although some limitations of the model were put in evidence.

However, being applied to periodic systems, the molecular EOPs were not able to reproduce the intensity of peaks in the polarized Raman spectra of α-quartz, especially in the low- and high-frequency spectral regions. The comparison of the molecular parameters with those derived from the periodic DFT calculations of silica polymorphs[17] indicates that values of the molecular α_L and α'_L parameters are larger than the corresponding values in the solids. The transversal α_T and α'_T components reveal a better transferability. Consequently, significantly larger anisotropies of the bond polarizability and its derivative in molecules are the primary reason of the above-mentioned discrepancy between the calculated and the experimental Raman spectra of α-quartz. It is supposed that the electric field of the solid is responsible for the variation of EOPs. If so, the parameters should be influenced by both the symmetry of the crystalline lattice and the degree of ionicity of chemical bonds. Further experimental and computational studies are necessary to verify this hypothesis.

Acknowledgment. We thank Dr. J. Laureyns for the recording of the polarized Raman spectra of α-quartz. The financial support of Indo-French Centre for the Promotion of Advanced Research (Project IFCPAR No. 3305-1) is gratefully acknowledged.

References and Notes

(1) Wolkenstein, M. W. *Compt. R. Acad. Sci. URSS* **1941**, *30*, 791.
(2) Long, D. A. *Proc. R. Soc. (London)* **1953**, *A217*, 203.
(3) Mayants, L. S.; Averbukh, B. S. *Theory and Calculation of Intensity in Vibrational Spectra of Molecules*; Nauka: Moscow, 1971.
(4) Murray, R. A.; Ching, W. Y. *Phys. Rev. B* **1989**, *39*, 1320.
(5) Zotov, N.; Ebbsjö, I.; Timmel, D.; Keppler, H. *Phys. Rev. B* **1999**, *60*, 6383.
(6) Umari P.; Pasquarello, A. *Physica B* **2002**, *316*−*317*, 572.
(7) Rahmani, A.; Benoit, M.; Benoit, C. *Phys. Rev. B* **2003**, *68*, 184202.
(8) Wu, Y. Q.; Jiang, G. C.; You, J. L.; Hou, H. Y.; Chen, H.; Xu, K. D. *J. Chem. Phys.* **2004**, *121*, 7883.
(9) Smirnov, K. S.; Bougeard, D. *J. Phys. Chem.* **1993**, *97*, 9434.
(10) Bornhauser, P.; Bougeard, D. *J. Raman Spectrosc.* **2001**, *32*, 279.
(11) Bougeard, D.; Smirnov, K. S.; Geidel, E. *J. Phys. Chem. B* **2000**, *104*, 9210.
(12) Arab, M.; Bougeard, D.; Smirnov, K. S. *Phys. Chem. Chem. Phys.* **2002**, *4*, 1957.
(13) Snoke, D. W.; Cardona, M. *Solid State Commun.* **1993**, *87*, 121.
(14) Thonhauser, T.; Mahan, G. D. *Phys. Rev. B* **2005**, *71*, 081307.
(15) Wu, G.; Zhou, J.; Dong, J. *Phys. Rev. B* **2005**, *72*, 115411.
(16) Feldman, J. L.; Singh, D. J.; Kendziora, C.; Mandrus, D.; Sales, B. C. *Phys. Rev. B* **2003**, *68*, 094301.
(17) Umari, P.; Pasquarello, A.; Dal Corso, A. *Phys. Rev. B* **2001**, *63*, 094305.
(18) Gussoni, M. In *Advances in Infrared and Raman Spectroscopy*; Clark, R. J. H.; Hester R. E. Eds.; Heyden & Son: London, 1980; Vol. 6, Chapter 2.
(19) Smirnov, K. S.; Bougeard, D. *J. Raman Spectrosc.* **2006**, *37*, 100.
(20) Wirtz, L.; Lazzeri, M.; Mauri, F.; Rubio, A. *Phys. Rev. B* **2005**, *71*, 241402.
(21) Frisch, M. J.; Trucks, G. W.; Schlegel, H. B.; Scuseria, G. E.; Robb, M. A.; Cheeseman, J. R.; Montgomery, J. A., Jr.; Vreven, T.; Kudin, K. N.; Burant, J. C.; Millam, J. M.; Iyengar, S. S.; Tomasi, J.; Barone, V.; Mennucci, B.; Cossi, M.; Scalmani, G.; Rega, N.; Petersson, G. A.; Nakatsuji, H.; Hada, M.; Ehara, M.; Toyota, K.; Fukuda, R.; Hasegawa, J.; Ishida, M.; Nakajima, T.; Honda, Y.; Kitao, O.; Nakai, H.; Klene, M.; Li, X.; Knox, J. E.; Hratchian, H. P.; Cross, J. B.; Bakken, V.; Adamo, C.; Jaramillo, J.; Gomperts, R.; Stratmann, R. E.; Yazyev, O.; Austin, A. J.; Cammi, R.; Pomelli, C.; Ochterski, J. W.; Ayala, P. Y.; Morokuma, K.; Voth, G. A.; Salvador, P.; Dannenberg, J. J.; Zakrzewski, V. G.; Dapprich, S.; Daniels, A. D.; Strain, M. C.; Farkas, O.; Malick, D. K.; Rabuck, A. D.; Raghavachari, K.; Foresman, J. B.; Ortiz, J. V.; Cui, Q.; Baboul, A. G.; Clifford, S.; Cioslowski, J.; Stefanov, B. B.; Liu, G.; Liashenko, A.; Piskorz, P.; Komaromi, I.; Martin, R. L.; Fox, D. J.; Keith, T.; Al-Laham, M. A.; Peng, C. Y.; Nanayakkara, A.; Challacombe, M.; Gill, P. M. W.; Johnson, B.; Chen, W.; Wong, M. W.; Gonzalez, C.; Pople, J. A. *Gaussian 03*, revision B.05: Gaussian, Inc.: Wallingford CT, 2004.
(22) Press: W. H.; Teukolsky, S. A.; Vetterling, W. T.; Flannery, B. P. *Numerical Recipes: The Art of Scientific Computing*. 2nd ed., Cambridge University Press: Cambridge, U.K., 1992.
(23) Le Page, Y.; Donnay, G. *Acta Crystallogr. B* **1976**, *32*, 2456.
(24) Lazarev, A. N.; Mirgorodsky, A. P. *Phys. Chem. Miner.* **1991**, *18*, 231.
(25) Gordon, R. G. *J. Chem. Phys.* **1965**, *42*, 3658.
(26) McQuarrie, D. A. *Statistical Mechanics*; Harper & Row: New York, 1976.
(27) Berens, P. H.; Wilson, K. R. *J. Chem. Phys.* **1981**, *75*, 515.
(28) Murphy, W. F. *J. Chem. Phys.* **1977**, *67*, 5877.
(29) Gough, K. M.; Dwyer, J. R.; Dawes, R. *Can. J. Chem.* **2000**, *78*, 1035.
(30) Badger, R. M. *J. Chem. Phys.* **1934**, *2*, 128.
(31) Ermoshin, V. A.; Smirnov, K. S.; Bougeard, D. *Chem. Phys.* **1996**, *202*, 53.
(32) Armstrong, R. S.; Clark, R. J. H. *J. Chem. Soc., Faraday Trans. 1* **1976**, *72*, 11.
(33) Lupinetti, C.; Gough, K. M. *J. Raman Spectrosc.* **2002**, *33*, 147.
(34) Spitzer, W. G.; Kleinman, D. A. *Phys. Rev.* **1961**, *121*, 1324.
(35) Gervais, F.; Piriou, B. *Phys. Rev. B* **1975**, *11*, 3944.
(36) Six normal modes with the vibrational frequencies below 100 cm^{-1} were excluded from the analysis. The zero-order BPM fails to describe the variation of the molecular polarizability in these modes, which comprise large-amplitude torsion and bending motions.
(37) Loudon, R. *Adv. Phys.* **1964**, *13*, 423.
(38) Scott, J. F.; Porto, S. P. S. *Phys. Rev.* **1967**, *161*, 903.
(39) Masso, J. D.; She, C. Y.; Edwards, D. F. *Phys. Rev. B* **1970**, *1*, 4179.
(40) Bermejo, D.; Montero, S.; Cardona, M.; Muramatsu, A. *Solid State Commun.* **1982**, *42*, 153.
(41) Guha, S.; Menéndez, J.; Page, J. B.; Adams, G. B. *Phys. Rev. B* **1996**, *53*, 13106.
(42) Rowell, R. L.; Stein, R. S. *J. Chem. Phys.* **1967**, *47*, 2985.
(43) Mortensen, E. M. *J. Chem. Phys.* **1968**, *49*, 3732.
(44) Applequist, J.; Carl, J. R.; Fung, K.-K. *J. Am. Chem. Soc.* **1972**, *94*, 2952.
(45) Silberstein, L. *Philos. Mag.* **1917**, *33*, 92, 521.
(46) Kanesaka, I.; Ikeda, S. *J. Raman Spectrosc.* **1992**, *23*, 181.
(47) Kanesaka, I.; Matsuda, T.; Niwa, Y. *J. Raman Spectrosc.* **1994**, *25*, 245.
(48) Pagnier, T.; Lucazeau, G. *J. Raman Spectrosc.* **1997**, *28*, 999.
(49) Kingma K. J.; Hemley, R. J. *Am. Mineral.* **1994**, *79*, 269−273. Database of Raman spectra: www.ens-lyon.fr/LST/Raman/spectrum.php?nom=quartz%20(powder).
(50) Armstrong, R. S.; Aroney, M. J.; Higgs, B. S.; Skamp, K. R. *J. Chem. Soc., Faraday Trans. 2* **1981**, *77*, 55.